Proceedings of BS2013:
13th Conference of International Building Performance Simulation Association, Chambéry, France, August 26-28

DEVELOPMENT OF A HIGH-ORDER DISCONTINUOUS GALERKIN METHOD FOR THE DNS AND LES OF NATURAL CONVECTION FLOWS IN BUILDINGS.

Koen Hillewaert, Corentin Carton de Wiart, Cécile Goffaux and Sébastien Pecceu
Cenaero, Rue des Frères Wright 29, B6041 Gosselies, Belgium

ABSTRACT

This paper discusses the use of a high-resolution code based on the discontinuous Galerkin method (DGM) for the *direct numerical simulation (DNS)* of natural convection flows in buildings. The high order of accuracy, combined to geometric flexibility and parallel scalability of DGM, provide - on paper - an ideal method for this type of simulation. Irrespective of whether this type of simulation is required for building design today, it is interesting to see already now how the DGM, compares to state of the art commercial solvers, as unsteady scale-resolving approaches will pervasive in the future. DGM computations on the ADNBATI benchmark are compared to DNS and URANS simulations performed by a state of the art commercial solver.

INTRODUCTION

Natural convection is driven by minute temperature and pressure differences, and usually features very complicated large scale unsteady flow patterns. When computing such flows, it is therefore very hard to predict where a fine grid resolution will be required, whilst high precision is required. Ideally Large Eddy Simulation (LES) or even direct numerical simulation (DNS) have to be used, which represent (part of) the turbulent structures directly. As unsteady Reynolds-Averaged Navier-Stokes approaches require a clear scale separation between turbulence and large scale unsteady features, these approaches are hence in theory not applicable. DNS and LES however require much higher computational resources than (U)RANS.

State of the art industrial solvers are based on low order discretisations. These methods have been very successful for the resolution of the RANS and URANS equations, which result in relatively slow and smooth flow patterns and hence fairly modest grid requirements. The high dissipation inherent to these methods is even an advantage, as it tends to stabilise the highly nonlinear character of the RANS equations.However, this dissipation, as well as the dispersion error will impact heavily on the ability to capture complex turbulent flow features using DNS and LES. This means that extremely well resolved meshes of high quality are needed for reliable quantitative predictions. Moreover, this mesh dependence may even impede a correct identification of critical zones for mesh refinement.

Currently, novel unstructured high-order accurate CFD discretisations are being developed. These solvers allow to obtain the precision of high-precision academic finite difference or spectral codes - dedicated to fundamental studies of turbulence - whilst providing the geometric flexibility of industrial methods. Of these methods, the *discontinuous Galerkin method (DGM)* is one of the most mature. Next to a very high degree of robustness with respect to mesh resolution and quality, this method provides an easy way of checking for adequate mesh resolution. It furthermore provides a solid mathematical background of adaptation strategies for both mesh size and interpolation order, in combination with the discretisation flexibility and robustness with mesh size transitions to allow for its practical implementation. This paves the way for automated computations in the long run.

Currently, Cenaero develops a new CFD code aimed at reliable large eddy simulation in complex geometry, based on a high-order DGM. It has already been validated for the direct numerical simulation and large eddy simulation of academic flows (Carton de Wiart et al., 2012b) as well as on more advanced configurations (Carton de Wiart et al., 2012a; Carton de Wiart and Hillewaert, 2012).

This paper discusses first results in the extension of the solver to natural convection of incompressible flows, aimed at studying building physics. Then, the method is applied on the ADNBATI case (http://adnbati.limsi.fr). Previous investigations performed with the commercial software ANSYS Fluent are presented. Finally, the case is computed using DGM and the results are compared to those obtained with Fluent.

THE ADNBATI BENCHMARK

Description and main conclusion

Designing energy efficient buildings require high thermal insulation as well as air tightness of the envelop, while the indoor air quality is assured by a mechanical or natural ventilation. Although this ventilation is primarily aimed to enhance the air quality, it can also be used for thermal management, *e.g.* by night free cooling. In order to avoid large discrepancies between the expected and the actual performance, the use of dynamic simulation tools can be a real asset. Currently 1D so-called *zonal models* are extensively used by architects while 3D *Computational Fluid Dynamics (CFD)* tools, known to be more accurate specifically when dealing with ventilation issues, are still reserved to research groups. The recent raise of the 3D mock-up use and of the Information and Communication Techniques (ICT) in the building community is however reducing the gap between the researchers and the engineering offices in terms of 3D simulation use.

In this context, the ADNBATI project (Pons et al., 2011, 2009) was launched to gather architects and re-

searchers around a night free cooling benchmark.
It is focused on a two-storey building consisting of a succession of rooms, symmetric two by two with respect to each separation wall, each of them opening directly to outdoor environment. It thus makes sense to simulate only one room. A schematic representation is given in Figure 1 where only the internal wall edges are shown for the sake of clarity. The room contains two non-symmetric sub-volumes (closet and bathroom) that make the geometry fully 3D. In addition to the two doors (East and West) and window (East), two opposite openings are especially designed for providing night free cooling: one under the window on the East side, one above the door on the West side.

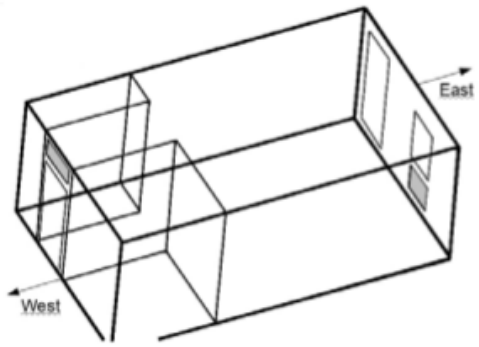

Figure 1: 3D sketch-up of the investigated room with internal edges (bold lines), internal subvolumes (intermediate lines) and openings (thin lines); the two openings designed for night free cooling are shown in grey

In order to decrease the computational cost and allow the participants to develop laboratory codes and then avoid to deal with a too large complexity, it was decided to reduce the benchmark to a 2D cavity with two openings. The objective was to assess the capacity of simulation tools to predict natural convection and the cross ventilation induced by a temperature difference between warm indoor air and walls and fresh outdoor air. This is a transient thermal problem where the heat transfer modes are coupled. However, it was decided to fix the wall temperatures, such that we are not constrained to solve the internal radiation, the conduction in the walls and the inertial response of the cavity walls. In terms of flow, we considered non-slip walls and non-reflecting conditions on the openings, with no additional wind pressure coefficients. The fluid convection was modeled with the Boussinesq approach.
A detailed description of the boundary conditions, the thermophysical properties of the fluid and a sketch of the reduced 2D cavity can be found in the reference (Pons et al., 2011).
Once the case study set up, the benchmark participants (Pons et al., 2011) developed their own codes or used commercial packages to assess the cooling rate and the cross ventilation mass flow. Analytical, semi-empirical, mono- and multi-zone (1D), Finite Element or Volume CFD (3D) models were tested.

Two values of the temperature difference between the walls and the outdoor air were investigated, 0.1 and $0.5°$C. Taking the room height (2.5m) as characteristic length, the Rayleigh numbers Ra were estimated, respectively, to $1.43\ 10^8$ and $7.15\ 10^8$.
These values of temperature difference are obviously much lower than realistic. This choice was done in order to reduce the numerical effort for the CFD models and also to maintain the rate of turbulence at a low level. High rates of turbulence make the notions of LES and DNS not fully relevant in 2D numerical simulations. With such values of Ra, the flow is likely to be unsteady but with a low turbulence intensity. LES, DNS, URANS and RANS turbulence modelling approaches were therefore compared in (Pons et al., 2011). In addition, grid sensitivity analyses were also performed.
The results of the benchmark highlighted that low fidelity methods (0D-1D) predict flow-rate rather well (20 percent inaccuracy), but cooling rate rather poorly (factor 2).
In this paper, we would like to follow up the benchmark effort by comparing the *Finite Volume Method (FVM)* CFD approach available in commercial packages to the *Discontinuous Galerkin Method (DGM)* developed by Cenaero for unsteady turbulent flow simulations. We will discuss mesh and turbulence approach issues. More specifically, we will demonstrate how DGM is promising to reduce the computational cost to perform high fidelity turbulence modeling in buildings and how it can ease the mesh generation close to the internal walls, to estimate correctly the heat transfer coefficient, which is usually a tricky operation and then a main concern of the building community dealing with CFD.

NUMERICAL METHOD

After an introduction to the model equations and the boundary conditions, the basic features of the discretisation is discussed, followed by validation results on a heated cavity.

Model equations

The flow is modeled by the Boussinesq approach, which solves for the incompressible perturbations of pressure head q', temperature T' and velocity $\mathbf{v}$ with respect to the ambient state, characterised by the temperature T_0, density ρ_0 and a hydrostatic variation of the static pressure around p_0. The density is linearized with respect to the temperature, as

$$\rho \approx \left(\rho_0 + \left(\frac{\partial \rho}{\partial T}\right)_p T'\right) = \rho_0 \left(1 - \beta_p T'\right) \qquad (1)$$

with β_p the thermal expansion coefficient at constant pressure. The pressure perturbation head with respect to the hydrostatic pressure then follows from $q' = (p - p_0)/\rho_0 - \mathbf{g} \cdot (\mathbf{x} - \mathbf{x}_0)$. Retaining only first order terms in the perturbations, the following set

of equations is found

$$\begin{aligned}\nabla \cdot \mathbf{v} &= 0\\ \frac{\partial \mathbf{v}}{\partial t} + \nabla \cdot \mathbf{v}\mathbf{v} + \nabla q' - \nabla \cdot \tau &= -\beta_p T' \mathbf{g}\\ \frac{\partial E'}{\partial t} + \nabla \cdot \mathbf{v} H' - \nabla \cdot \mathbf{v} \cdot \tau - \nabla \cdot \kappa \nabla T' &= -\beta_p T' \mathbf{g} \cdot \mathbf{v}\end{aligned} \tag{2}$$

completed by the constitutive equations

$$\begin{aligned}\beta_p &= -\frac{1}{\rho_0}\left(\frac{\partial \rho}{\partial T}\right)_p = \frac{1}{T_0}\\ H' &= E' + q' = c_v T' + q'\\ \tau &= \nu\left(\nabla \mathbf{v} + \nabla \mathbf{v}^T\right)\end{aligned} \tag{3}$$

with c_v the specific heat capacity at constant volume, ν the kinematic viscosity, and κ the heat conductivity. Hereby the fluid is assumed to behave as an ideal gas.

Time-integration and iterative strategy

The pseudo-compressibility approach is used. For simplicity, the set of equations is rewritten as a generic set of convection-diffusion-source equations for the state vector $\tilde{u}$ defined on domain Ω.

$$\begin{aligned}\mathbf{P}_{mn}\frac{\partial \tilde{u}_n^{k+1}}{\partial \tau} + \frac{\partial \tilde{w}_m}{\partial t}\\ + \nabla \cdot \mathbf{f}_m(\tilde{u}) + \nabla \cdot \mathbf{d}_m(\tilde{u}, \nabla \tilde{u}) + \mathcal{S}_m = 0\ ,\ \forall m\end{aligned} \tag{4}$$

m is the index running on the variables in the primitive state vector $\tilde{u}$ and the vector of conserved quantities $\tilde{w}$

$$\begin{aligned}\tilde{u} &= \begin{bmatrix} q' & \mathbf{v} & T' \end{bmatrix}^T\\ \tilde{w} &= \begin{bmatrix} 0 & \mathbf{v} & E' \end{bmatrix}^T\end{aligned} \tag{5}$$

whilst $\mathbf{f}$, $\mathbf{d}$ and $\mathcal{S}$ are respectively the convective and the diffusive flux vectors and $\mathcal{S}$ the source term vector. The preconditioning matrix $\mathbf{P}$ is defined as

$$\mathbf{P} = \begin{bmatrix} \frac{1}{c^2} & 0 & 0 & 0\\ \frac{v_x}{c^2} & 1 & 0 & 0\\ \frac{v_x}{c^2} & 0 & 1 & 0\\ \frac{H'}{c^2} & v_x & v_y & C_v \end{bmatrix} \tag{6}$$

The physical time derivative in the equation 4 is discretised by the three point backward difference scheme. For each physical time step t^k the following equations

$$\begin{aligned}\mathbf{P}_{mn}\frac{\partial \tilde{u}_n^k}{\partial \tau} + \frac{3u^k - 4u^{k-1} + u^{k-2}}{2\Delta t}\\ + \nabla \cdot \mathbf{f}_m(\tilde{u}^k) + \nabla \cdot \mathbf{d}_m(\tilde{u}^k, \nabla \tilde{u}^k) + S_m = 0\ ,\ \forall m\end{aligned} \tag{7}$$

is iterated onto "steady" state in the pseudo time τ. For unsteady computations, the pseudo-time step $\Delta\tau = \infty$. The preconditioning matrix then only appears in the discretisation of the convective terms, as detailed in the following section. This formulation is based on a modified version of the methods proposed by Turkel (1987); previously a similar method has been applied to DGM by Bassi et al. (2007).

The discontinuous Galerkin method

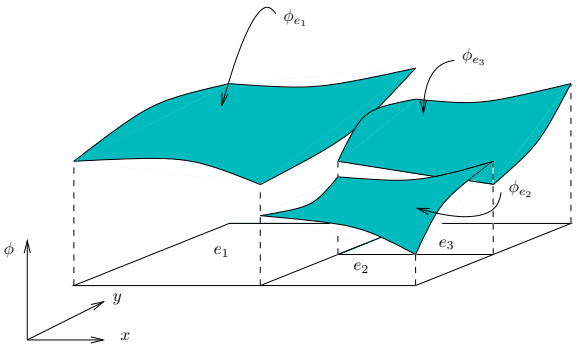

Figure 2: A non-conforming discontinuous Galerkin interpolation on a mesh composed of quadrilaterals

The discontinuous Galerkin method (DGM) ((Cockburn et al., 2000; Arnold et al., 2002)) is a Galerkin finite element method based on a "broken" interpolation space $\mathcal{V}$, composed of functions ϕ that are high-order polynomials on each of the elements e in the mesh, but not required to be continuous across the interfaces f between elements. Such an interpolant has been illustrated in Figure 2. The DGM then approximates component m of the solution state vector $\tilde{u}$ by u as

$$u_m = \sum_i \mathbf{u}_{im}\phi_i\ ,\ \phi_i \in \mathcal{V}$$

As for any Galerkin method, $\mathbf{u}_{im}$ are found by requiring that the residual of the model equations, evaluated with u, is orthogonal to any function ϕ_j within $\mathcal{V}$. This principle is complemented with interface terms to ensure stability and convergence. A comprehensive review of the formulations for the diffusive terms can be found in (Arnold et al., 2002).

Each interface is oriented following the choice of its normal $\mathbf{n}$. Using $+$ and $-$ to indicate values of u approaching the interface respectively following and opposite of the interface normal $\mathbf{n}$, as well as the signed normals $\mathbf{n}^- = \mathbf{n}$ and $\mathbf{n}^+ = -\mathbf{n}$. With these conventions interface average $\langle . \rangle$ and jump $[[.]]$ operators are defined as

$$\begin{aligned}\langle a \rangle &= (a^+ + a^-)/2\\ [[a]] &= a^-\mathbf{n}^- + a^+\mathbf{n}^+\end{aligned} \tag{8}$$

For the convective discretisation the standard discontinuous Galerkin method is used, based on the definition of a convective interface flux $\mathcal{H}$ which will be discussed subsequently. The diffusive terms are discretised with the *Symmetric Interior Penalty (SIP)*

method, leading to the variational formulation

$$
\begin{aligned}
&\forall \phi_i \in \mathcal{V}\ ,\ \forall m: \\
&\sum_e \int_e \phi_i \frac{\partial u_m}{\partial t} dV \\
&- \sum_e \int_e \nabla \phi_i \cdot (\mathbf{f}_m + \mathbf{d}_m)\, dV \\
&\underbrace{+ \sum_f \int_f [[\phi_i]] \cdot \mathbf{n}\, \mathcal{H}_m \left(u^+, u^-, \mathbf{n}\right) dS}_{CI} \\
&\underbrace{+ \sum_f \int_f [[\phi_i]]^k \langle \mathcal{D}^{kl}_{mn} \cdot \frac{\partial u_n}{\partial x^l} \rangle dS}_{DI} \\
&\underbrace{+ \sum_f \int_f [[u_n]]^k \langle \mathcal{D}^{kl}_{nm} \cdot \frac{\partial \phi_i}{\partial x^l} \rangle dS}_{DS} \\
&\underbrace{+ \sum_f \sigma \int_f [[u_m]] \cdot [[\phi_i]] dS}_{DP} = 0
\end{aligned}
$$

which has to be satisified for all ϕ_i in the base of $\mathcal{V}$ and every variable m. Hereby it is assumed that the diffusive fluxes $\mathbf{d}$ depend as follows on the solution and its gradients

$$\mathbf{d}^k_m = \mathcal{D}^{kl}_{mn}(u) \frac{\partial u_n}{\partial x^l}$$

The interface convective flux $\mathcal{H}$ is chosen based on the Lax-Friedrichs approximate Riemann solver $\mathcal{H}^*$ for the preconditioned system in pseudo-time

$$
\begin{aligned}
&\frac{\partial u_m}{\partial \tau} + \mathbf{P}^{-1}_{mn} (\nabla \cdot \mathbf{f}_n) = 0 \\
&\mathcal{H}^*_m = \mathbf{P}^{-1}_{mn} (\mathbf{f}_n \cdot \mathbf{n} + \lambda^*_{\max} ([[u]]_n \cdot \mathbf{n}))
\end{aligned}
\tag{9}
$$

where $\lambda^*_{\max}$ is the absolute value of the largest eigenvalue of the matrix $\mathbf{F}^*$

$$\mathbf{F}^*_{mn} = \mathbf{P}^{-1}_{mk} \frac{\partial}{\partial u_n} (\mathbf{f}_k \cdot \mathbf{n}) \tag{10}$$

and finally

$$\mathcal{H}_m = \mathbf{P}_{mn} \mathcal{H}^*_n \tag{11}$$

where $\mathbf{f}$, $\mathbf{P}$, $\mathbf{F}^*$ and λ^* have been evaluated at $u = \langle u \rangle$. All Dirichlet boundary conditions, both for the convective and diffusive equations are imposed weakly by providing a fictitious exterior state for the convective interface flux terms **CI**, the consistent diffusive flux **DI**, the symmetrising term **DS** and the penalty term **DP**. Neumann boundary conditions for the diffusive terms are enforced by modifying the consistent DI and symmetrising term DS on the concerned faces.

Reinterpretation

A very instructive way to reinterpret the method is to consider it as a collection of Galerkin finite element problems defined per element, weakly coupled through internal boundary conditions. For the convective terms, the interface flux $\mathcal{H}$ assures the physically correct transport of characteristics sent to and received from neighboring cells, thus assuring correctly posed elementwise problems and global energy stability. For the diffusive terms the method generalises a boundary penalty method to enforce weak coupling at the interfaces. The penalty parameter σ can be freely chosen, but should be large enough to guarantee stability. This choice is not as arbitrary as would appear at first sight, since sharp bounds for the value of σ have been elaborated for all mesh types ((Shahbazi, 2005; Hillewaert et al., 2012)).

Validation on the heated cavity

The natural convection cell in a square heated cavity of varying size W has been studied by (Barakos et al., 1994), mainly to illustrate the impact of turbulence modeling.

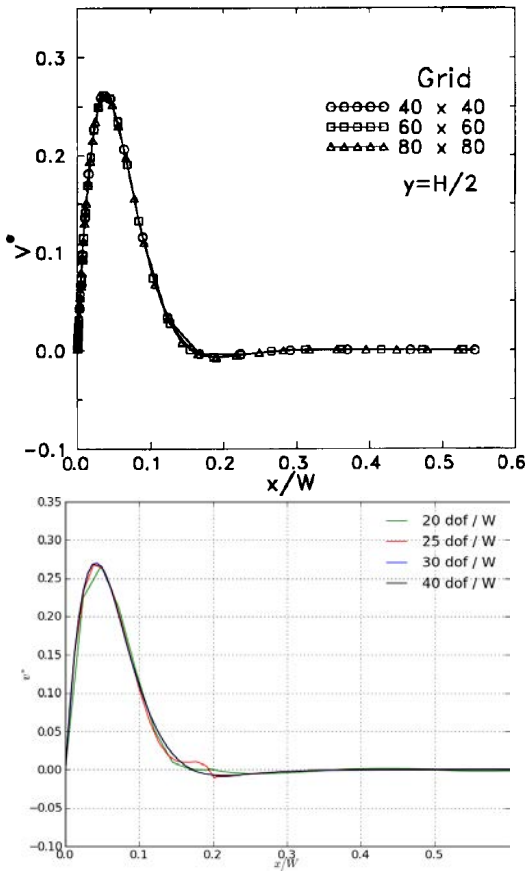

Figure 3: Spanwise variation of the vertical velocity computed by Barakos et al. (top) and current (bottom) for $Ra = 10^6$.

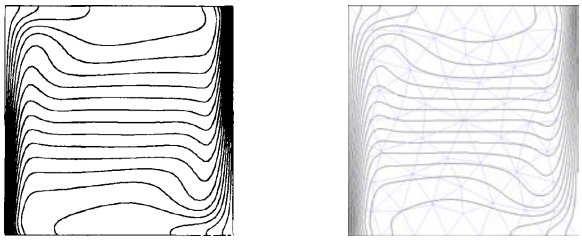

Figure 4: Variation of the temperature computed by Barakos et al. (top) and current with a resolution of 30 dof/W (bottom).

The flow is heated at $T_0 + \Delta/2$ and cooled to $T_0 - \Delta T/2$ on the west and east wall respectively, whilst the north and south wall are adiabatic. An interesting result of this study is that RANS models introduced an important source of error for laminar flow regimes, with a marked tendency to smear out temperature variations and boundary layers.
To validate the method, this test case was computed for $Ra = 10^6$. The working fluid is air at standard conditions (*i.e.* $p_0 = 101325$ Pa and $T_0 = 293.15$ K, the chamber size is $W = 7.81$ cm and the temperature difference between the two walls is $\Delta T = 20$ K.
Figure 3 compares the variation of the non-dimensionalised vertical velocity $v_y/\sqrt{g\beta\Delta TW}$ as a function of the non-dimensional distance x/W along a horizontal cut at mid-height. To ease the comparison, the number of degrees of freedom (*i.e.* number of cells times order interpolant order) along the width of the chamber, is indicated. Although very decent agreement is obtained at 20 dof/W, the velocity profile is grid-converged for 30 dof/W, whereas the minimal resolution for the finite volume computation is said to be 40 dof/W, following (Barakos et al., 1994). Moreover, the grid is not structured and does not feature any boundary layer zones. Figure 4 shows the isolines of the temperature, together with the mesh corresponding to a resolution of 30 dof/W. Remark that the isolines of the reference FVM computation are not fully symmetric.

ADNBATI RESULTS

Figure 5 shows the different mesh resolutions that have been used during both the DGM and FVM simulations. The so-called *coarse* mesh is isotropic and does not feature any boundary layer next to the wall (with a $7.5\ cm$ characteristic size, excepted close to the openings where a grid refinement was performed till $5\ cm$). We added a boundary layer in the *baseline* case (with a off-wall height of $1\ cm$). The last so-called *fine* is defined by a $1\ cm$ surface and volume characteristic size and a off-wall height of $0.3\ cm$ in the boundary layer.

(U)RANS computations with a Finite Volume commercial package

A first series of simulations was performed with the commercial software ANSYS Fluent (ANS, 2009), which is based on a finite volume formulation of the Navier-Stokes equations. The turbulence was modeled by the Reynolds Averaged Navier Stokes (RANS) approach, which requires the least computational effort. In that approach, the turbulent structures are not computed but their averaged impact on the mean flow is modeled, whilst additional equations are added to provide the characterisation and evolution of the turbulence. Different models exist and some of them are compared in this work (the Spalart-Allmaras, the $k-\epsilon$ model and the $k-\omega$ models).
We set up the model following the boundary conditions and the flow model prescribed in the ADNBATI benchmark, for a temperature difference of 0.5 °C between the walls and the outdoor. Note that, for all the calculations, second order numerical schemes were chosen to discretize the equations in space and time.

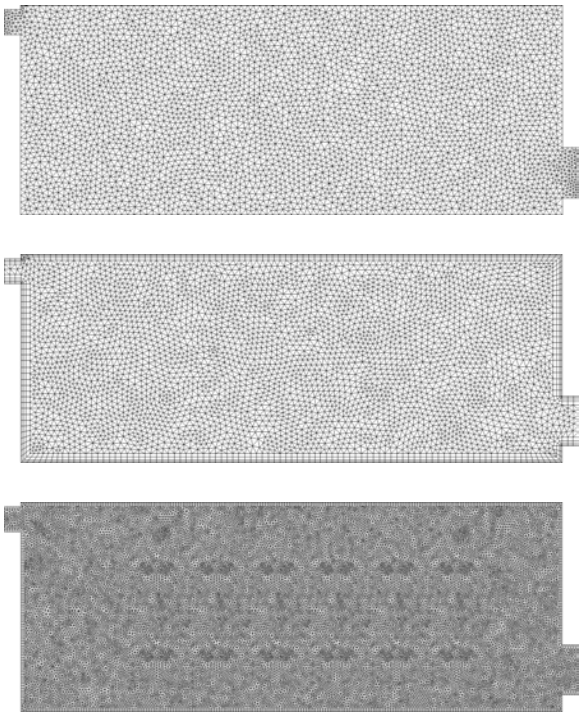

Figure 5: Mesh resolutions used for the simulation - from top to bottom coarse, baseline and fine.

Since the flow is transient, the RANS ($k-\omega$ model) approach encountered some troubles to converge, given a moderate and oscillating residual values, inducing oscillating state values and cross ventilation mass flow rate. This mass flow, averaged on a thousand of iterations, oscillates around 50.0 m^3/h and is bound between 47.5 and 52.5 m^3/h. Figure 6 (top part) shows the temperature field within the room for this RANS calculation, get on the so-called *baseline* mesh, previously introduced. Even if the result is not converged, the result looks physical -or at least realistic- in terms of flow and thermal stratification.
We therefore moved to an Unsteady RANS (URANS) simulation, with a temporal resolution of 1 second. An instantaneous temperature field is shown on Figure 6 (bottom). Figure 7 shows the mass flow rate time evolution, starting from an homogeneous hot temperature

within the room and on the walls (25.5°C and 25°C outside). The evolution of the mass flow rate for the three RANS models mentioned above is compared in Figure 7, till on the baseline mesh.

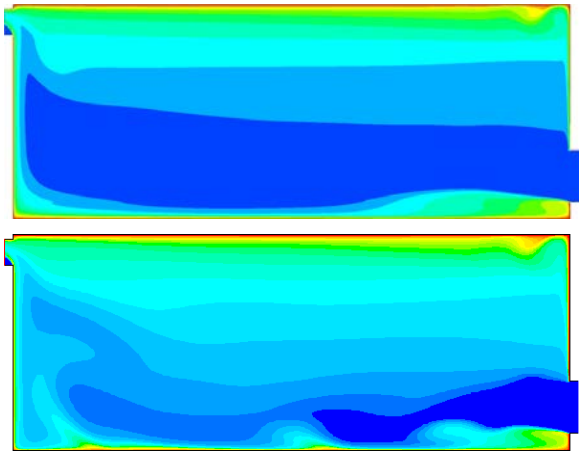

Figure 6: Temperature field for a temperature difference of 0.5 °C between internal walls and outdoor obtained by a RANS calculation (top) and a URANS (bottom) calculation after 2000 seconds. Both results are obtained using the $k-\omega$ model on the baseline mesh. Temperature levels are shown every 0.05°C between 25°C and 25.5°C

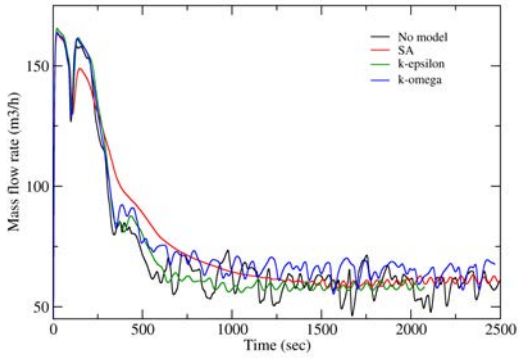

Figure 7: Mass flow time evolution for a temperature difference of $0.5°C$ between internal walls and outdoor obtained by URANS (Spalart Almaras(SA), $k-\epsilon$ and $k-\omega$ models), TNS ($No\ model$) simulations. The results are obtained on the baseline mesh.

We notice two peaks in the mass flow in the first stage of the time evolution, corresponding to the massive entry of fresh air, falling to the ground and then reflecting to the wall opposite to the entry. After this transition, the mass flow finally oscillates in time, due to the fact the internal walls are artificially kept at a constant and hotter temperature, so that the ventilation can not cool them, explaining the sustained regime. The mass flow was averaged on the last 1500 time steps to give a value of 57 m^3/h, which is not so far from the RANS averaged value (the relative error is close to ten percent). This suggests that the RANS approach can be of real interest in a pre-design stage since it gives a result very quickly (less than 5 minutes in this 2D case, on a single processor).

In Figure 7, the URANS results are furthermore compared to those obtained by a *Truncated Numerical Simulation (TNS)* (ie. a transient computation without any turbulence model) This result is to be considered with caution, given the choice for a 2D simulation - incompatible with truely turbulent flows - and the relatively coarse mesh resolution. It is interesting to notice that all the tested methods in Fluent converged to the same averaged mass flow value. Obviously minor differences are seen in the oscillation about this average, which can be attributed to a difference in the capture of local physics, in particular the formation and size of local convection cells. Most noticeably the Spalart-Almaras model smoothes the fluctuations significantly, as does - to a lesser extent - the $k-\epsilon$ model, known to be more viscous and better suited to deal with jet flow modeling.

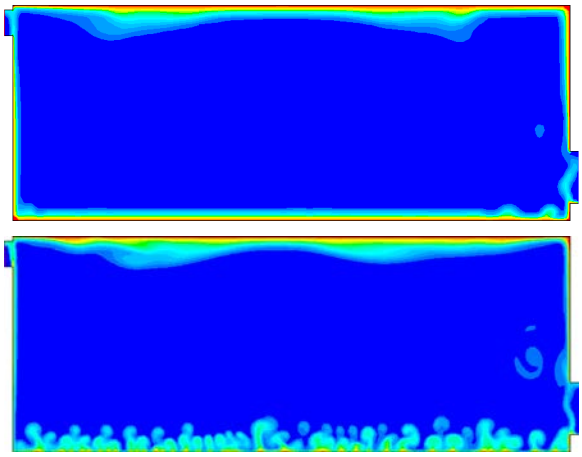

Figure 8: Temperature field after 100 seconds, starting from a homogeneous air temperature in the room and outside (25°C). The top view is obtained on the so-called coarse mesh and the bottom view for a much more detailed mesh (the fine mesh). Temperature levels are shown every 0.05°C between 25°C and 25.5°C

To confirm these results, a mesh convergence study was performed. We distinguish two grid refinement parameters: the off-wall height of the first boundary layer element (for a fixed 1.2 grow rate and global thickness) and the isotropic cell size on the boundaries and in the room. As previously said, the above simulations were achieved on the baseline case, which leads to a URANS run taking half a day in a single processor. We tested several meshes, from 0.2 to 15 cm for the first cell in the boundary layer, and 2 to 20 cm in terms of surface and volume mesh. We also made some tests without boundary layer (isotropic mesh). Note that we kept a minimum mesh size of 5 cm close the inlets and outlets due to their small dimensions.

The mass flow is only dependent on the boundary layer features, provided the surface and the volume mesh size is equal or smaller than 20 cm, which is obvi-

sously coarse at the room scale. This is due to the fact that the wall heat transfer coefficient, acting as the crucial parameter in this case, is known to be strongly grid sensitive with no suited wall function available in the commercial package we used. Mesh convergence is reached once the first cell size is equal of lower than 1 cm. From 1 to 7.5 cm, the relative error on the mass flow estimate increases till 15 per cent, which could still however be acceptable in a pre-design stage.

Nervetheless, as for the choice of the turbulence model, both boundary layer and volume mesh features impact the local and the time-dependent flow profile within the room. In that sense, a grid independence was found when both boundary layer first cell and volume mesh size is equal or lower than 1 cm. For example, Figure 8 compares the convection cells within the room after 100 seconds, starting from an homogeneous and equal temperature between the room air and the outdoor (25°C) and hot walls (25.5°C) for two different meshes: the so called *coarse* and *fine* meshes introduced above. The physical details area clearly better captured in the refined case.

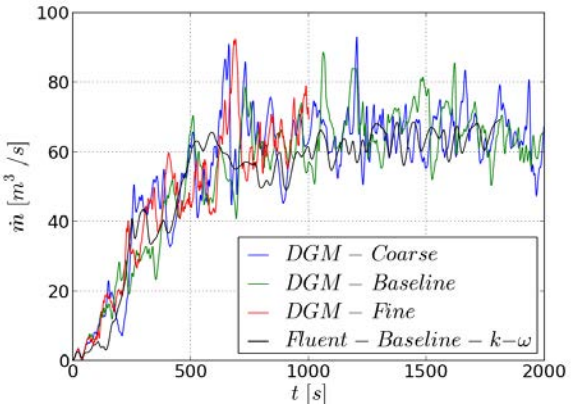

Figure 9: Comparison of the evolution of the mass flow in the room in the ADNBATI test case computed with the 4^{th} order accurate DGM on all meshes, to the results obtained by the FVM computations using a k-ω model.

As a conclusion, the turbulence model choice does not seem to be the dominant factor with respect to the average mass flow rate for this particular problem. Some discrepancies appear which must be related to the local physics captured in the room. Moreover, the steady RANS approaches seem to provide a reasonable assessment of the mass flow rate. On the other hand, the wall heat transfer coefficient must be sufficiently well estimated to avoid large discrepancy which means that a boundary layer is necessary, with a first layer thickness of about 1 cm. This is an important remark from a practical point of view since the boundary layer generation becomes a tricky matter in 3D and in a real building configuration.

Obviously these conclusions in terms of turbulence models, time approach and grid sensitivity should be investigated at higher Rayleigh number and in three dimensions.

DNS computations using DGM solver

The computations were undertaken with a 4th order accurate version of the DGM code, on the meshes shown in Figure 5. It should be noted that the actual resolution is about 3 times finer than for the finite volume method, due to the degrees of freedom inside of each element.

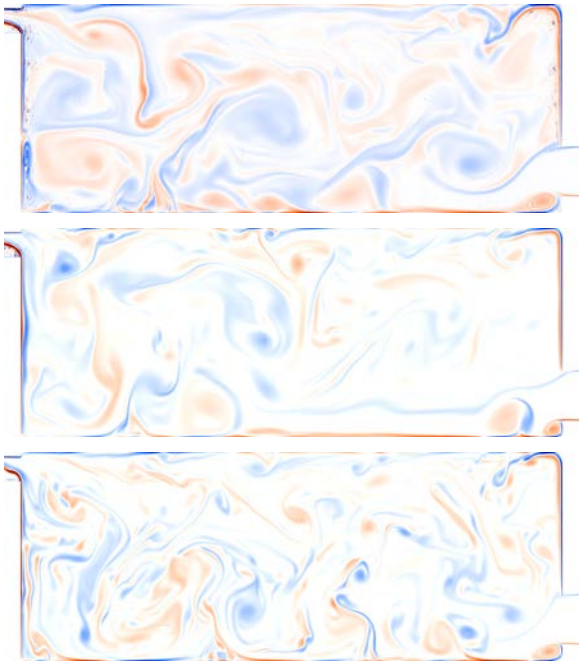

Figure 10: Snapshots of vorticity field computed by DGM once the flow regime is established. From top to bottom: coarse, baseline and fine mesh.

The mass flow rate evolution, compared to the Fluent (k-ω URANS on the baseline mesh) computations is given in Figure 9. Remark that the initial condition of these simulations was chosen to be $25°C$ within the room, such as the outdoor temperature. All of the DGM computations give the correct time-average mass flow rate.

The main criterion for assessing the resolution of the computation, is the continuity of the computed vorticity, as shown in Figure 10. This quantity is based on solution derivatives and is hence more difficult to converge than the solution variables itself. One can clearly see that even for the coarsest mesh only in zones of very high shear, such as in the outlet and wall boundary layers, minor discontinuities can be seen. This means that these computations are resolved on the baseline and finest mesh, and nearly fully resolved on the coarsest.

CONCLUSION

A novel CFD code based on the discontinous Galerkin method is being developed for reliable LES and DNS computations in complex geometry. This paper has illustrated its capacities to model natural convection

problems with a high fidelity.
The method has been compared on the ADNBATI benchmark with the commercial solver ANSYS Fluent, based on finite volume approach. The ADNBATI benchmark focuses on the numerical simulation of the night free cooling of a simplified room. Previous validations on Fluent have shown that the turbulence model choice has a negligible impact on the global mass flow of fresh air crossing the room. Nevertheless, a grid sensitivity study has shown that the mass flow is strongly impacted by the off-wall height with a convergence reached once it is equal or lower than 1 cm, so that the wall heat transfer coefficient is accurately estimated. This can be easily and efficiently done in this 2D case by using a boundary layer approach in the meshing stage but can appear much more tricky when dealing with a complex 3D building case.
Therefore, the DGM approach sounds as a promising approach to overcome this issue since we have found very accurate results without boundary layer and with a rather isotropic mesh based on a charactertic size several times larger than 1 cm. It opens the way to an easier 3D-based design to non-expert operators, since the mesh operation could be easily automated, and to a stronger integration and interoperability of 3D CAE tools and 3D CAO tools used by both researchers and engineering and/or architect offices.

ACKNOWLEDGMENTS

We would like to thank the participants of the *ADNBATI* benchmark for the interesting and valuable discussions. The ADNBATI project was supported by the *Programme Interdisciplinaire Énergie* of the CNRS (PE ADNBATI #PE09-3.2.1-1), and the *ANR-Habitat Intelligent et Solaire Photovoltaïque* programme (project 4C #ANR-08-HABISOL- 019). Cenaero's work was partially achieved in the frame of the SIMBA project, supported by the Walloon Region and the ERDF.

REFERENCES

2009. *ANSYS Fluent 13.0 Documentation*.

Arnold, D., Brezzi, F., Cockburn, B., and Marini, L. 2002. Unified Analysis of Discontinuous Galerkin Methods for Elliptic Problems. *SIAM J. Num. Anal*, 39:1749–1779.

Barakos, G., Mitsoulis, E., and Assimacopoulos, D. 1994. Natural convection flow in a square cavity revisited: laminar and turbulent models with wall functions. *Int. J. Num. Fluids*, 18:695–719.

Bassi, F., Crivellini, A., Pietro, D. A. D., and Rebay, S. 2007. An implicit high-order discontinuous galerkin method for steady and unsteady incompressible flows. *Computers & Fluids*, 36(10):1529 – 1546.

Carton de Wiart, C. and Hillewaert, K. 2012. DNS and ILES of transitional flows around a SD7003 airfoil using a high order Discontinuous Galerkin Method. In *Seventh International Conference on Computational Fluid Dynamics (ICCFD7)*, Big Island, Hawaii.

Carton de Wiart, C., Hillewaert, K., and Geuzaine, P. 2012a. DNS of a Low Pressure Turbine Blade computed with the Discontinuous Galerkin Method (asme-gt2012-68900). In *ASME Turbo Expo 2012 Turbine Technical Conference and Exposition*, Copenhagen, Denmark. ASME.

Carton de Wiart, C., Hillewaert, K., Geuzaine, P., Luccioni, R., Bricteux, L., Coussement, G., and Winckelmans, G. 2012b. Assessment of LES modeling within a high order Discontinuous Galerkin solver. In *Proceedings of ETMM9*, Thessaloniki, Greece.

Cockburn, B., Karniadakis, G., and Shu, C.-W. 2000. The development of discontinuous Galerkin methods. In Cockburn, B., Karniadakis, G. E., and Shu, C.-W., editors, *Discontinuous Galerkin Methods*, pages 3–50. Springer.

Hillewaert, K., Remacle, J.-F., and Drosson, M. 2012. Sharp constants in the hp-finite element trace inverse inequality for standard functional spaces on all element types in hybrid meshes. *In review fo the SIAM Journal on Numerical Analysis*.

Pons, M., Bastide, A., Brangeon, B., Wurtz, E., Stephan, L., Goffaux, C., Jay, A., Maalouf, C., and Salagnac, P. 2009. *Amélioration de la Description Numérique du Bâtiment, Projet exploratoire du Programme Interdisciplinaire ENERGIE du CNRS*. http://adnbati.limsi.fr.

Pons, M., Bastide, A., Brangeon, B., Wurtz, E., Stephan, L., Goffaux, C., Jay, A., Maalouf, C., and Salagnac, P. 2011. The test case adnbati, a benchmark on natural ventilation in a room. In *Fifth International Conference on Advanced COmputational Methods in ENgineering (ACOMEN 2011)*, Liège, Belgium.

Shahbazi, K. 2005. An explicit expression for the penalty parameter of the interior penalty method (Short note). *Journal of Computational Physics*, 205:401–407.

Turkel, E. 1987. Preconditioned methods for solving the incompressible and low speed compressible equations. *J. Comp. Phys.*, 72:277–298.